8th International Conference on Computational and Mathematical Biomedical Engineering - CMBE2024
24–26 June 2024, USA
P. Nithiarasu and R. Löhner (Eds.)

EFFICIENT NUMERICAL SCHEMES FOR UNCERTAINTY QUANTIFICATION IN DIFFEOMORPHIC IMAGE REGISTRATION GOVERNED BY TRANSPORT EQUATIONS

Jae Youn Kim and Andreas Mang
Department of Mathematics, University of Houston, andreas@math.uh.edu

SUMMARY

We present effective numerical schemes for solving initial value control problems for diffeomorphic image registration. Our formulation is governed by a transport equation for the image intensities and the Euler–Poincaré equation associated with the group of diffeomorphisms. We present effective numerical methods for the evaluation of forward and adjoint operators. We propose fast numerical schemes to approximate the covariance matrix of the posterior distribution for uncertainty quantification. Our applications are in biomedical imaging.

Key words: *diffeomorphic registration, uncertainty quantification, PDE-constrained optimization*

1 INTRODUCTION

Image registration is a non-linear, ill-posed inverse problem. Generally speaking, image registration is about establishing a *plausible* spatial correspondence $y \in \mathcal{Y}$, $\mathcal{Y} \subseteq \{\phi \mid \phi : \mathbb{R}^d \to \mathbb{R}^d\}$ between two (or more) images $m_1 : \bar{\Omega} \to \mathbb{R}_{\geq 0}$ (the "reference image") and $m_0 : \bar{\Omega} \to \mathbb{R}_{\geq 0}$ (the "template image") of the same object or scene, such that the deformed template image becomes similar to the reference image [12, 13]. The images are defined as compactly supported function on an open set $\Omega \subset \mathbb{R}^d$ (with $d \in \{2, 3\}$), with closure $\bar{\Omega} := \Omega \cup \partial\Omega$ and boundary $\partial\Omega$. In our work, we limit the set $\mathcal{Y}$ of admissible transformations to $\mathbb{R}^d$-diffeomorphisms, i.e., smooth maps that are one-to-one, onto, and have a smooth inverse. One way to guarantee that y is a diffeomorphism is to introduce a pseudo-time variable $t \in [0, 1]$ and parameterize y in terms of a smooth, time-dependent velocity field $v \in L^2([0, 1], \mathcal{H})$ [11, 14–16, 19]. Given v, the map y represents the endpoint of the flow equation $\partial_t \phi = v \circ \phi$ for $t \in (0, 1]$ with initial condition $\phi = \mathrm{id}_{\mathbb{R}^d}$ at time $t = 0$, where $\mathrm{id}_{\mathbb{R}^d}(x) = x$ for any $x \in \mathbb{R}^d$ is the identity transformation. For suitable choices of the Sobolev space $\mathcal{H} = W^{p,s}(\Omega, \mathbb{R}^d)$, $p \in \mathbb{N}$, $s \in \mathbb{N}$, the map y is guaranteed to be a diffeomorphism [14, 16, 19]. In our formulation, we do not model the transformation of the template image m_0 by applying the map y; we directly transport the intensities of m_0 given v [6–8, 10]. This leads to a PDE-constrained optimization problem.

Contributions. In the present work, we extend our past work on numerical methods for PDE-constrained formulations for diffeomorphic image registration [6–8, 10]. In particular, we introduce an additional PDE constraint—the Euler–Poincaré equation associated with the group of diffeomorphisms (EPDiff) [20, 21]. We describe efficient numerical schemes for the evaluation of the forward and adjoint operators. We use low-rank approximations based on randomized algorithms [24, 25] to construct the Hessian. We estimate uncertainties based on curvature information [27, 28].

Related Work. This work extends our past efforts to design fast algorithms for diffeomorphic image registration [1–10]. Related works on PDE-constrained formulations for diffeomorphic image registration include [17, 22]. Examples for works that consider the EPDiff equation are [18, 23, 26, 30]. The works closest to ours are [26, 30].

2 METHODS

Problem Formulation. The constraints for our problem are a hyperbolic transport equation for the image intensities of m_0 and the EPDiff equation for the momentum $u \in L^2([0,1], \mathcal{H}^*)$. The variational problem is as follows: Given two images m_0 and m_1 we seek the initial momentum $u_0 \in \mathcal{H}^*$ by solving

$$\underset{v,u,m,u_0}{\text{minimize}} \quad \frac{1}{2}\int_\Omega (m(t=1,x), m_1(x))^2 \,\mathrm{d}x + \frac{\alpha}{2}\int_\Omega \langle \mathcal{K}u_0, u_0\rangle_{\mathbb{R}^d} \,\mathrm{d}x \tag{1a}$$

$$\text{subject to} \quad c(m,u,v,u_0) = 0. \tag{1b}$$

The state variables of (1) are the space-time fields $u : [0,1] \times \bar{\Omega} \to \mathbb{R}^d$, $v : [0,1] \times \bar{\Omega} \to \mathbb{R}^d$, and $m : [0,1] \times \bar{\Omega} \to \mathbb{R}$. The control or decision variable is $u_0 : \bar{\Omega} \to \mathbb{R}^d$. The first term in (1a) is a squared L^2-distance that measures the proximity between the transported image intensities of m_0 at $t = 1$ and the reference image m_1. The second term in (1a) is a Tikhonov-type regularization functional with $\mathcal{K} : \mathcal{H}^* \to \mathcal{H}, \mathcal{K} = \mathcal{L}^{-1}$, where $\mathcal{L} : \mathcal{H} \to \mathcal{H}^*$, $\mathcal{L} := \alpha_1 \operatorname{diag}(\Delta^2, \dots, \Delta^2) - \alpha_2 \operatorname{diag}(\Delta, \dots, \Delta) + \alpha_3 \operatorname{id}_{\mathbb{R}^d}$. We fix the parameters $\alpha_i > 0$ and only vary the regularization parameter $\alpha > 0$. We select $\alpha_1 = $ 1e–1 and $\alpha_2 = \alpha_3 = 1$. The constraint c in (1b) is given

$$\partial_t m + \nabla m \cdot v = 0 \qquad \text{in } (0,1] \times \Omega, \tag{2a}$$

$$m - m_0 = 0 \qquad \text{in } \{0\} \times \Omega, \tag{2b}$$

$$\partial_t u + (\nabla v)^\mathsf{T} u + (\nabla u) v + u(\nabla \cdot v) = 0 \qquad \text{in } (0,1] \times \Omega, \tag{2c}$$

$$u - u_0 = 0 \qquad \text{in } \{0\} \times \Omega, \tag{2d}$$

$$v - \mathcal{K}u = 0 \qquad \text{in } [0,1] \times \Omega, \tag{2e}$$

with periodic boundary conditions on $\partial\Omega$. For a given (candidate) velocity field v, (2a) models the transport of the image intensities of m_0. The velocity field v is found by solving the EPDiff equation (2c) for a (candidate) initial momentum u_0.

Numerical Methods. We use an *optimize-then-discretize* approach. That is, we form the Lagrangian of (1) and derive the optimality conditions in the continuum using variational calculus. Subsequently, we discretize the resulting system of equations. We use a pseudo-spectral discretization in space. We discretize integral operators based on a midpoint rule. We use a semi-Lagrangian method for time integration and a globalized Gauss–Newton–Krylov method fo optimization.

Uncertainty Quantification. Our approach uses ideas described in [26–30]. Our goal is to design efficient numerical schemes to estimate the covariance $C_{\text{post}} \succ 0$ of the posterior distribution π_{post} of u_0 conditioned on the data m_1. To this end, we consider a reduced formulation of (1). That is, we introduce the *parameter-to-observation* map $\mathcal{F}$, which represents the solution operator of (2). This enables us to reformulate (1) as an unconstrained optimization problem and establishes a direct connection between (1) and the negative log posterior $\ell(u_0) := -\log \pi_{\text{post}}(u_0 \,|\, m_1)$. According to Bayes theorem, $\pi_{\text{post}}(u_0 \,|\, m_1) \propto \pi_{\text{like}}(m_1 \,|\, u_0)\, \pi_{\text{prior}}(u_0)$. Here, π_{like} is the likelihood and π_{prior} denotes the prior, which correspond to the distance and regularization functional in (1), respectively. With slight abuse of notation we assume all quantities have been discretized. Under the assumption that the map $\mathcal{F}$ is linear, it can be shown that π_{post} is a Gaussian distribution with a covariance that corresponds to the Hessian $H \succ 0$ of ℓ [28]. Since $\mathcal{F}$ is not linear, we use a quadratic approximation (i.e., a linearization) of the negative log posterior. Consequently, in our nonlinear setting the inverse of the Hessian H is only an approximation of C_{post}. We obtain

$$C_{\text{post}} \approx H^{-1} = (H_{\text{dat}} + H_{\text{reg}})^{-1} = H_{\text{reg}}^{1/2}(H_{\text{reg}}^{1/2} H_{\text{dat}} H_{\text{reg}}^{1/2} + I)^{-1} H_{\text{reg}}^{1/2},$$

where H_{dat} denotes the contribution of the data part of our problem and $H_{\text{reg}} \succ 0$ denotes the regularization part. We note that we do not form or store H; our algorithm is matrix-free. We use a randomized algorithms [24, 25] to compute a rank r approximation of $H_{\text{reg}}^{1/2} H_{\text{dat}} H_{\text{reg}}^{1/2}$. Using the Sherman–Morrison–Woodbury identity, we obtain

$$(H_{\text{reg}}^{1/2} H_{\text{dat}} H_{\text{reg}}^{1/2} + I)^{-1} \approx (V_r S_r V_r^\mathsf{T} + I)^{-1} = I - V_r (S_r^{-1} + I)^{-1} V_r^\mathsf{T}.$$

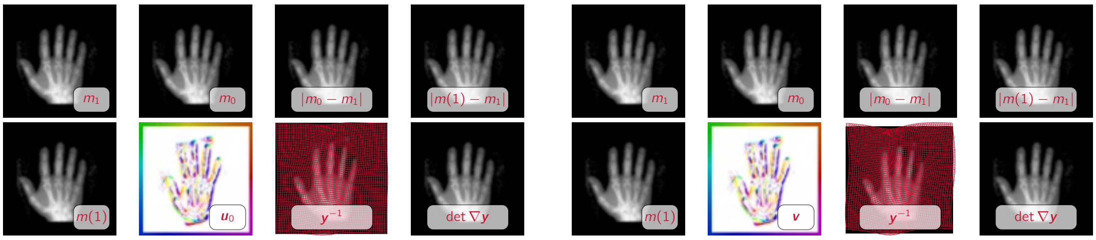

Figure 1: Registration results. Left block: new problem formulation. Right block: old problem formulation [10]. We consider a dataset from [12] of size 128×128. Top row for each block (from left to right): reference image m_1, template image m_0, and residual differences before and after registration. Bottom row (from left to right): deformed template image, computed initial momentum u_0/velocity v (color denotes orientation), illustration of the associated map y^{-1}, and determinant of the deformation gradient $\det \nabla y$.

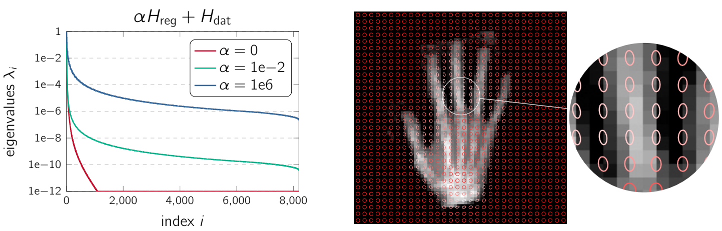

Figure 2: Left: Spectrum of the Hessian for different regularization parameters α. Right: Local estimates of the posterior covariance matrix entries visualized as ellipsoids. Uncertainties are pronounced along edges and reduced perpendicular to those edges.

3 RESULTS AND CONCLUSIONS

We show exemplary registration results in Figure 1. We show the spectrum of the Hessian in Figure 2 (left). We show local estimates of the posterior covariance entries in Figure 2 (right).

We have presented effective numerical schemes for solving PDE-constrained optimization problems for diffeomorphic image registration governed by a transport equation and the EPDiff equation. The variational problem belongs to the class of initial value control problems. We have developed an effective numerical framework that allows us to estimate local uncertainties based on curvature information of the negative log posterior.

Acknowledgements. This work was partly supported by the National Science Foundation (NSF) through the grants DMS-2009923 and DMS-2012825. Any opinions, findings, and conclusions or recommendations expressed herein are those of the authors and do not necessarily reflect the views of the NSF.

REFERENCES

[1] A. Mang. CLAIRE: Scalable GPU-accelerated algorithms for diffeomorphic image registration in 3D. *Applied and Numerical Harmonic Analysis*, Springer, 2024.

[2] M. Brunn, N. Himthani, G. Biros, M. Mehl, and A. Mang. CLAIRE: Constrained large deformation diffeomorphic image registration on parallel computing architectures. *The Journal of Open Source Software*, 6(61), 3038, 2021.

[3] M. Brunn, N. Himthani, G. Biros, M. Mehl, and A. Mang. Fast GPU 3D diffeomorphic image registration. *Journal of Parallel and Distributed Computing*, 149:149–162, 2021.

[4] M. Brunn, N. Himthani, G. Biros, M. Mehl and A. Mang. Multi-node multi-GPU diffeomorphic image registration for large-scale imaging problems. Proc ACM/IEEE Conference on Supercomputing, pp. 523–539, 2020.

[5] A. Mang, A. Gholami, C. Davatzikos, and G. Biros. CLAIRE: A distributed-memory solver for constrained large deformation diffeomorphic image registration. *SIAM Journal on Scientific Computing*, 41(5):C548–C584, 2019.

[6] A. Mang and G. Biros. A semi-Lagrangian two-level preconditioned Newton–Krylov solver for constrained diffeomorphic image registration. *SIAM Journal on Scientific Computing*, 39(6):B1064–B1101, 2017.

[7] A. Mang and L. Ruthotto. A Lagrangian Gauss–Newton–Krylov solver for intensity- and mass-preserving diffeomorphic image registration. *SIAM Journal on Scientific Computing*, 39(5):B860–B885, 2017.

[8] A. Mang and G. Biros. Constrained H^1-regularization schemes for diffeomorphic image registration. *SIAM Journal on Imaging Sciences*, 9(3):1154–1194, 2016.

[9] A. Mang, A. Gholami, and G. Biros. Distributed-memory large-deformation diffeomorphic 3D image registration. Proc ACM/IEEE Conference on Supercomputing, pp. 842–853, 2016.

[10] A. Mang and G. Biros. An inexact Newton–Krylov algorithm for constrained diffeomorphic image registration. *SIAM Journal on Imaging Sciences*, 8(2):1030–1069, 2015.

[11] A. Mang, J. He, and R. Azencott. An operator-splitting approach for variational optimal control formulations for diffeomorphic shape matching. *Journal of Computational Physics*, 493:112463, 2023.

[12] J. Modersitzki. *FAIR: flexible algorithms for image registration*. Society for Industrial and Applied Mathematics, 2009.

[13] B. Fischer and J. Modersitzki. Ill-posed medicine—an introduction to image registration. *Inverse Problems*, 24(3):034008.

[14] A. Trouvé. Diffeomorphism groups and pattern matching in image analysis. *International Journal of Computer Vision* 28(3):213–221, 1998.

[15] M. F. Beg, M. I. Miller, A. Trouvé, and L. Younes. Computing large deformation metric mappings via geodesic flows of diffeomorphisms. *International Journal of Computer Vision*, 61:139–157, 2005.

[16] P. Dupuis, U. Gernander, and M. I. Miller. Variational problems on flows of diffeomorphisms for image matching. *Quarterly of Applied Mathematics*, 56(3):587–600, 1998.

[17] A. Borzi, K. Ito, and K. Kunisch. Optimal control formulation for determining optical flow. *SIAM Journal on Scientific Computing* 24(3):818–847, 2002.

[18] L. Younes, F. Arrate, and M. I. Miller. Evolutions equations in computational anatomy. *NeuroImage* 45:S40–S50, 2009.

[19] L. Younes. *Shapes and diffeomorphisms*. Springer, 2019.

[20] V. I. Arnold. Sur la géométrie différentiell des gropues de Lie de dimension infine et ses applications al'hydrodynamique des fluides parfaits. *Annales de l'Institut Fourier* 16:319–361, 1966.

[21] V. I. Arnold. Les méthods mathématiques de la méchanique classique. MIR, Moscow, 1976.

[22] G. L. Hart, C. Zach, and M. Niethammer. An optimal control approach for deformable registration. Proc IEEE Conference on Computer Vision and Pattern Recognition. pp. 9–16, 2009.

[23] M. I. Miller, A. Trouvé, and L. Younes. Geodesic shooting for computational anatomy. *Journal of Mathematical Imaging and Vision*, 24:209–228, 2006.

[24] N. Halko, P. G. Martinsson, and J. A. Tropp. Finding structure in randomness: Probabilistic algorithms for constructing approximate matrix decompositions. *SIAM Review*, 53(2):217–288, 2010.

[25] P.-G. Martinsson and J. A. Tropp. Randomized numerical linear algebra: Foundations and algorithms. *Acta Numerica* 29:403–572, 2020.

[26] X. Yang and M. Niethammer. Uncertainty quantification for LDDMM using low-rank Hessian approximation. Proc Medical Image Computing and Computer-Assisted Intervention. Vol. LNCS 9350. 2015, 289–296.

[27] T. Bui-Thanh, O. Ghattas, J. Martin, and G. Stadler. A computational framework for infinite-dimensional Bayesian inverse problems: The linearized case, with application to global seismic inversion. *SIAM Journal on Scientific Computing*, 35(6):A2494–A2523, 2013.

[28] J. Martin, L. C. Wilcox, C. Burstedde, and O. Ghattas. A stochastic Newton MCMC method for large-scale statistical inverse problems with application to seismic inversion. *SIAM Journal on Scientific Computing*, 34(3):A1460–A1487, 2012.

[29] A. M. Stuart. Inverse problems: A Bayesian perspective. *Acta Numerica* 19:451–559, 2010.

[30] Wang, J., Wells III, W. M., Golland, P., and Zhang, M. Registration uncertainty quantification via low-dimensional characterization of geometric deformations. Magnetic Resonance Imaging, 64:122–131, 2019.